

Supporting information for:

Intermolecular π -hole / $n \rightarrow \pi^*$ interactions with carbon monoxide ligands in crystal structures

Michael Timothy Doppert, Hannah van Overeem and Tiddo J. Mooibroek*

van 't Hoff Institute for Molecular Sciences, Universiteit van Amsterdam
Science Park 904, 1098 XH Amsterdam, The Netherlands
E-mail: t.j.mooibroek@uva.nl

Figure S1	Orbital overlap between n and π^* orbitals of the dme adducts shown in Figure 1.....	2
Figure S2	Distribution of M in M-CO structures.....	3
Figure S3	Distribution of M in $M(\text{CO})_3$ structures.....	4
Figure S4	Query used to construct the model of $M(\text{CO})_3$ structures.....	5
Figure S5	Perspective views of aligned structured involving $M(\text{CO})_3$ fragments.....	6
Figure S5	AIM analyses of examples highlighted in Figure 4.....	7
Table S1	Cartesian coordinates of optimized structures shown in Figure 1.....	8
Table S2	Numerical and topological analysis of carbon monoxide ligands present in the.....	9
Table S3	Numerical overview of the nature of EIR of the data used in Figure 3.....	10
Table S4	Computational evaluation of the complexes highlighted in Figure 4 and Figure	11

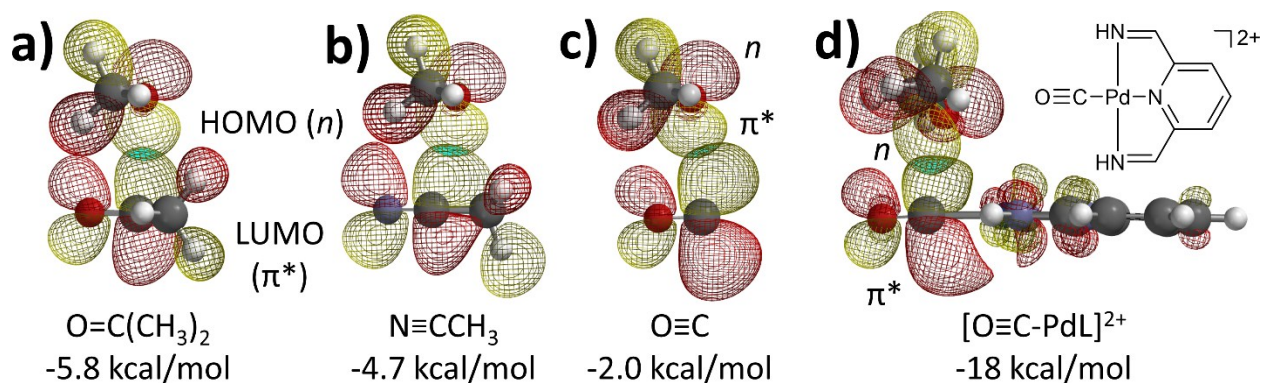


Figure S1. Ball and stick representations with selected (n / π^*) orbitals of complexes with dimethyl ether (dme, always on top) and acetone (a), acetonitrile (b), carbon monoxide (c) and a carbon monoxide ligand in a Palladium-pyridine-2,6-diylidimethanimine complex. The areas highlighted in green indicate orbital overlap. In the Palladium complex (d) the n and π^* orbitals are delocalized over both molecular fragments. Geometry optimizations and energy computations were performed at the DFT/B3LYP-D3/def2-TZVP level of theory.[‡] See for Cartesian coordinated Table S1 and see Figure 1 for an ‘atoms in molecules analysis’. A fragment analysis with ADF at the B3LYP-D3/TZ2P level of theory (no frozen cores and scalar relativity) was also performed, revealing a pauli repulsion of: 6.87 (a), 4.95 (b), 2.43 (c) and 15.5 (d) kcal/mol; an electrostatic attraction of: -5.43 (a), -4.56 (b), -1.45 (c) and -17.1 (d) kcal/mol; orbital interactions of: -2.21 (a), -1.51 (b), -0.84 (c) and -11.0 (d) kcal/mol; and dispersion energies of: -4.94 (a), -3.40 (b), -1.90 (c) and -5.17 (d) kcal/mol.

¹ H 0% 0																	² He 0% 0
³ Li 0% 0	⁴ Be 0% 0											⁵ B 0% 0	⁶ C 0% 0	⁷ N 0% 0	⁸ O 0% 0	⁹ F 0% 0	¹⁰ Ne 0% 0
¹¹ Na 0% 0	¹² Mg 0% 0											¹³ Al 0% 0	¹⁴ Si 0% 0	¹⁵ P 0% 0	¹⁶ S 0% 0	¹⁷ Cl 0% 0	¹⁸ Ar 0% 0
¹⁹ K 0% 0	²⁰ Ca 0% 0	²¹ Sc 0% 0	²² Ti 0% 80	²³ V 0.1% 265	²⁴ Cr 6.5% 15560	²⁵ Mn 6.1% 14429	²⁶ Fe 18.4% 43920	²⁷ Co 7.3% 17473	²⁸ Ni 0.6% 1366	²⁹ Cu 0.1% 156	³⁰ Zn 0% 0	³¹ Ga 0% 0	³² Ge 0% 0	³³ As 0% 0	³⁴ Se 0% 0	³⁵ Br 0% 0	³⁶ Kr 0% 0
³⁷ Rb 0% 0	³⁸ Sr 0% 0	³⁹ Y 0% 0	⁴⁰ Zr 0% 46	⁴¹ Nb 0.1% 197	⁴² Mo 6.1% 14591	⁴³ Tc 0.2% 423	⁴⁴ Ru 18.3% 43583	⁴⁵ Rh 1.9% 4502	⁴⁶ Pd 0% 51	⁴⁷ Ag 0% 16	⁴⁸ Cd 0% 12	⁴⁹ In 0% 0	⁵⁰ Sn 0% 0	⁵¹ Sb 0% 0	⁵² Te 0% 0	⁵³ I 0% 0	⁵⁴ Xe 0% 0
⁵⁵ Cs 0% 0	⁵⁶ Ba 0% 0	⁵⁷ La's 0% 0	⁷² Hf 0% 5	⁷³ Ta 0.1% 138	⁷⁴ W 8.6% 20594	⁷⁵ Re 9.4% 22306	⁷⁶ Os 13.9% 33154	⁷⁷ Ir 1.8% 4364	⁷⁸ Pt 0.5% 1132	⁷⁹ Au 0% 9	⁸⁰ Hg 0% 1	⁸¹ Tl 0% 0	⁸² Pb 0% 0	⁸³ Bi 0% 0	⁸⁴ Po 0% 0	⁸⁵ At 0% 0	⁸⁶ Rn 0% 0
⁸⁷ Fr 0% 0	⁸⁸ Ra 0% 0	⁸⁹ Ac's 0% 0	¹⁰⁴ Rf 0% 0	¹⁰⁵ Db 0% 0	¹⁰⁶ Sg 0% 0	¹⁰⁷ Bh 0% 0	¹⁰⁸ Hs 0% 0	¹⁰⁹ Mt 0% 0	¹¹⁰ Ds 0% 0	¹¹¹ Rg 0% 0	¹¹² Cn 0% 0	¹¹³ Uut 0% 0	¹¹⁴ Fl 0% 0	¹¹⁵ Uup 0% 0	¹¹⁶ Lv 0% 0	¹¹⁷ Uus 0% 0	¹¹⁸ Uuo 0% 0
⁵⁷ La 0% 0	⁵⁸ Ce 0% 5	⁵⁹ Pr 0% 0	⁶⁰ Nd 0% 0	⁶¹ Pm 0% 0	⁶² Sm 0% 0	⁶³ Eu 0% 0	⁶⁴ Gd 0% 0	⁶⁵ Tb 0% 0	⁶⁶ Dy 0% 0	⁶⁷ Ho 0% 0	⁶⁸ Er 0% 0	⁶⁹ Tm 0% 0	⁷⁰ Yb 0% 0	⁷¹ Lu 0% 0			
⁸⁹ Ac 0% 0	⁹⁰ Th 0% 0	⁹¹ Pa 0% 0	⁹² U 0% 0	⁹³ Np 0% 0	⁹⁴ Pu 0% 0	⁹⁵ Am 0% 0	⁹⁶ Cm 0% 0	⁹⁷ Bk 0% 0	⁹⁸ Cf 0% 0	⁹⁹ Uut 0% 0	¹⁰⁰ Fl 0% 0	¹⁰¹ Uup 0% 0	¹⁰² Lv 0% 0	¹⁰³ Uus 0% 0			

Figure S2. Schematic representation of the distribution of metals coordinated by a carbon monoxide ligand. The data represents 251,262 M---C≡O structures found within 48,019 CIFs (see also entry 1 in Table S1). The color code is meant as a guide to the eye, where red is the highest percentage of data, then green and light blue the lowest.

¹ H 0 % 0																	² He 0 % 0
³ Li 0 % 0	⁴ Be 0 % 0											⁵ B 0 % 0	⁶ C 0 % 0	⁷ N 0 % 0	⁸ O 0 % 0	⁹ F 0 % 0	¹⁰ Ne 0 % 0
¹¹ Na 0 % 0	¹² Mg 0 % 0											¹³ Al 0 % 0	¹⁴ Si 0 % 0	¹⁵ P 0 % 0	¹⁶ S 0 % 0	¹⁷ Cl 0 % 0	¹⁸ Ar 0 % 0
¹⁹ K 0 % 0	²⁰ Ca 0 % 0	²¹ Sc 0 % 0	²² Ti 0.1 % 76	²³ V 0.2 % 247	²⁴ Cr 14.7 % 17138	²⁵ Mn 7.3 % 8538	²⁶ Fe 11.9 % 13901	²⁷ Co 3.9 % 4523	²⁸ Ni 0.1 % 75	²⁹ Cu 0 % 6	³⁰ Zn 0 % 0	³¹ Ga 0 % 0	³² Ge 0 % 0	³³ As 0 % 0	³⁴ Se 0 % 0	³⁵ Br 0 % 0	³⁶ Kr 0 % 0
³⁷ Rb 0 % 0	³⁸ Sr 0 % 0	³⁹ Y 0 % 0	⁴⁰ Zr 0 % 22	⁴¹ Nb 0.1 % 66	⁴² Mo 6 % 7022	⁴³ Tc 0.2 % 287	⁴⁴ Ru 8.6 % 10065	⁴⁵ Rh 0 % 39	⁴⁶ Pd 0 % 4	⁴⁷ Ag 0 % 0	⁴⁸ Cd 0 % 4	⁴⁹ In 0 % 0	⁵⁰ Sn 0 % 0	⁵¹ Sb 0 % 0	⁵² Te 0 % 0	⁵³ I 0 % 0	⁵⁴ Xe 0 % 0
⁵⁵ Cs 0 % 0	⁵⁶ Ba 0 % 0	⁵⁷ ₇₁ La's 0 % 10	⁷² Hf 0 % 0	⁷³ Ta 0 % 49	⁷⁴ W 23.3 % 27141	⁷⁵ Re 10.9 % 12694	⁷⁶ Os 12.3 % 14301	⁷⁷ Ir 0.2 % 208	⁷⁸ Pt 0 % 4	⁷⁹ Au 0 % 0	⁸⁰ Hg 0 % 0	⁸¹ Tl 0 % 0	⁸² Pb 0 % 0	⁸³ Bi 0 % 0	⁸⁴ Po 0 % 0	⁸⁵ At 0 % 0	⁸⁶ Rn 0 % 0
⁸⁷ Fr 0 % 0	⁸⁸ Ra 0 % 0	⁸⁹ ₁₀₃ Ac's 0 % 0	¹⁰⁴ Rf 0 % 0	¹⁰⁵ Db 0 % 0	¹⁰⁶ Sg 0 % 0	¹⁰⁷ Bh 0 % 0	¹⁰⁸ Hs 0 % 0	¹⁰⁹ Mt 0 % 0	¹¹⁰ Ds 0 % 0	¹¹¹ Rg 0 % 0	¹¹² Cn 0 % 0	¹¹³ Uut 0 % 0	¹¹⁴ Fl 0 % 0	¹¹⁵ Uup 0 % 0	¹¹⁶ Lv 0 % 0	¹¹⁷ Uus 0 % 0	¹¹⁸ Uuo 0 % 0
			⁵⁷ La 0 % 0	⁵⁸ Ce 0 % 10	⁵⁹ Pr 0 % 0	⁶⁰ Nd 0 % 0	⁶¹ Pm 0 % 0	⁶² Sm 0 % 0	⁶³ Eu 0 % 0	⁶⁴ Gd 0 % 0	⁶⁵ Tb 0 % 0	⁶⁶ Dy 0 % 0	⁶⁷ Ho 0 % 0	⁶⁸ Er 0 % 0	⁶⁹ Tm 0 % 0	⁷⁰ Yb 0 % 0	⁷¹ Lu 0 % 0
			⁸⁹ Ac 0 % 0	⁹⁰ Th 0 % 0	⁹¹ Pa 0 % 0	⁹² U 0 % 0	⁹³ Np 0 % 0	⁹⁴ Pu 0 % 0	⁹⁵ Am 0 % 0	⁹⁶ Cm 0 % 0	⁹⁷ Bk 0 % 0	⁹⁸ Cf 0 % 0	⁹⁹ Uut 0 % 0	¹⁰⁰ Fl 0 % 0	¹⁰¹ Uup 0 % 0	¹⁰² Lv 0 % 0	¹⁰³ Uus 0 % 0

Figure S3. Schematic representation of the distribution of metals coordinated by a carbon monoxide ligand in $M(CO)_3$ structures (see also Figure Sx). The data represents 113,065 $M(C\equiv O)_3$ structures (45% of all $M\text{---}C\equiv O$ structures) found within 28,597 CIFs (60% of all $M\text{---}C\equiv O$ containing CIFs, see also entry 7 in Table S1). The color code is meant as a guide to the eye, where red is the highest percentage of data, then green and light blue the lowest.

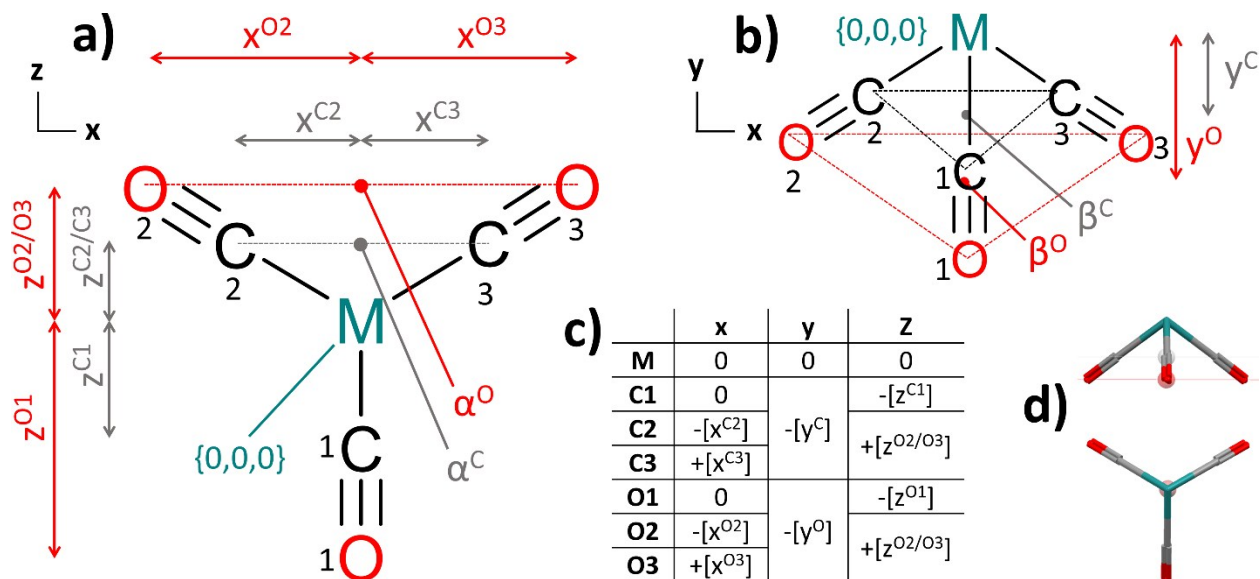


Figure S4. Schematic representation of the query used to construct the model of $M(\text{CO})_3$ structures as viewed along the y -axis (a) and the z -axis (b). Using the measurement defined in (a) and (b), the cartesian coordinates of the model are represented in the table in (c) with the measured values being as follows: $x^{C2} = x^{C3} = 1.374 \pm 0.074 \text{ \AA}$; $x^{O2} = x^{O3} = 2.194 \pm 0.120 \text{ \AA}$; $y^C = 1.021 \pm 0.172 \text{ \AA}$; $y^O = 1.651 \pm 0.266 \text{ \AA}$; $z^{C1} = 1.585 \pm 0.088 \text{ \AA}$; $z^{C2/C3} = 0.793 \pm 0.044 \text{ \AA}$; $z^{O2/O3} = 1.266 \pm 0.071 \text{ \AA}$; $z^{O1} = 2.532 \pm 0.143 \text{ \AA}$. The reconstructed model is shown in (d) along the z -axis (top) and y -axis (bottom). In the query, all C-M-C angles were constrained to $\leq 140^\circ$ to exclude trans-coordinated CO ligands and M could be any metal (see also Figure 2). The measurements for the model were taken from 76,959 structures found within 27,305 CIFs.

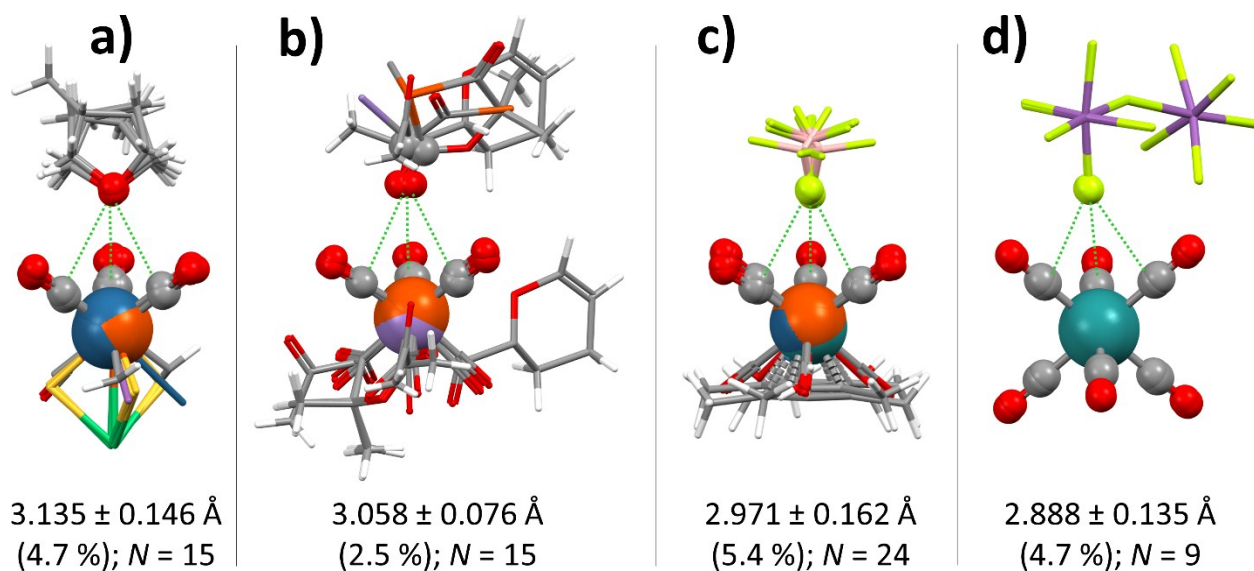


Figure S5. Perspective views with associated average distances of aligned structures involving $M(\text{CO})_3$ fragments in close contact with sp^3 hybridized O-atoms (a), sp^2 hybridized O-atoms (b), BF_4^- anions (c) and $\text{Sb}_2\text{F}_{11}^-$ anions (d). Alignments were conducted in PyMOL using the pair fitting wizard. The structures used in (a) were MOPZUO, NOFRUW (3 distinct fragments) and VEWKED; in (b) were ACUZII, ACUZII01, HIDSIW, PYRMNC and QENCOC; in (c) were CEHHIH, CEHHON, CUWYOW, CUWYOW01 (two distinct fragments), DUSYIZ, GOZYOJ and VOTJAP; and in (d) were HOLMOK, LARPIE and LARPOK. The average van der Waals overlap in each cases is 0.085 \AA (a); 0.162 \AA (b); 0.199 \AA (c); 0.285 \AA (d). See Table S4 for single point energy computations.

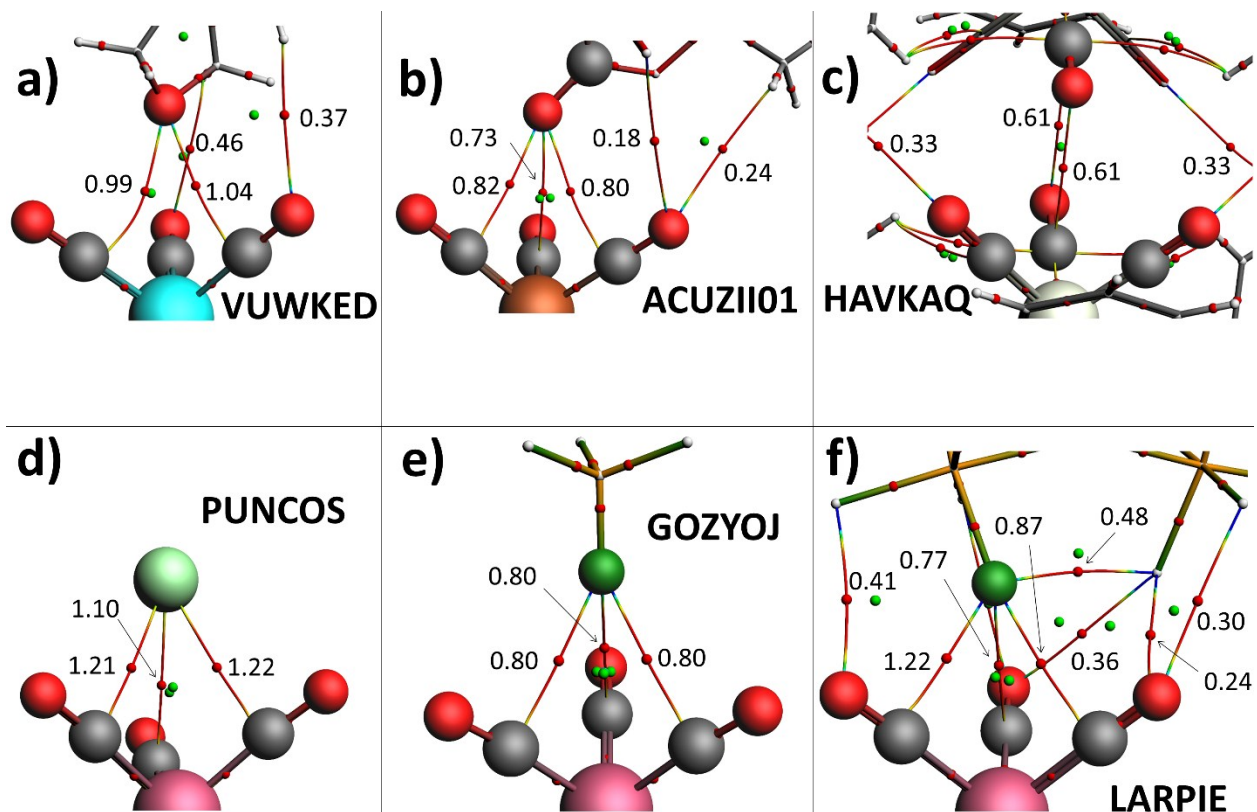


Figure S5. Perspective views of ball and stick representations with selected bond critical points (ρ in 10^{-2} x a.u., small red dots), ring critical points (small green dots) and bond paths (thin lines) of the complexes highlighted in Figure 4. Calculations were conducted with ADF at the B3LYP-D3/TZ2P level of theory (no frozen cores and scalar relativity), except for HAVKAQ (c), which was computed at the GGA:BP-D3(BK)/DZ level of theory due to the large cluster involved. **NB:** Note that in all cases the most dense bond critical points involve a C-atom of a CO ligand and the interacting electron rich atom (O, Cl, or F).

Table S1. Cartesian coordinates of the geometry optimized structures shown in Figure 1. Computations were done with the density functional theorem at the B3LYP-D3/def2-TZVP level of theory. For references purposes, a methane dimer was computed with $\Delta E = -0.570$ kcal/mol (not shown).

[O=C(CH ₃) ₂ ...O(CH ₃) ₂] (Figure 1a) $\Delta E = -5.830$ kcal/mol				[N=CCH ₃ ...O(CH ₃) ₂] (Figure 1b) $\Delta E = -4.701$ kcal/mol				[O=C...O(CH ₃) ₂] (Figure 1c) $\Delta E = -2.042$ kcal/mol			
X	Y	Z		X	Y	Z		X	Y	Z	
C	-0.2448	-1.1768	-1.7583	C	-1.0680	0.0026	2.0131	C	-2.6772	0.0606	-0.8452
C	-0.2463	1.1735	-1.7587	C	0.3473	-1.1767	-1.3083	C	0.6423	-1.1356	0.0101
C	0.4042	-1.2810	1.6416	C	0.3843	0.0002	1.9457	C	0.5229	1.2126	0.0506
C	-0.3670	0.0023	1.4326	C	0.3442	1.1742	-1.3057	H	-0.0676	-1.2503	0.8400
C	0.4064	1.2837	1.6457	H	0.5973	1.2349	-2.3725	H	1.6613	-1.1414	0.4197
H	0.7970	-1.3242	2.6608	H	1.2683	1.2200	-0.7175	H	0.5291	-1.9772	-0.6723
H	-0.4346	-1.2189	-2.8389	H	-0.2830	-2.0279	-1.0505	H	-0.1666	1.2087	0.9057
H	-1.2004	-1.2368	-1.2239	H	1.2713	-1.2214	-0.7199	H	0.2864	2.0593	-0.5926
H	0.3769	-2.0263	-1.4772	H	0.6008	-1.2345	-2.3752	H	1.5468	1.3262	0.4313
H	0.3736	2.0238	-1.4763	H	-1.4624	-0.8748	1.5022	O	-2.6656	-0.4047	0.1802
H	-1.2027	1.2317	-1.2257	H	-1.4596	0.8858	1.5102	O	0.3882	0.0418	-0.7274
H	-0.4345	1.2159	-2.8396	H	-1.3969	-0.0012	3.0528	[O=C...O(CH ₃) ₂] in THF (implicit)			
H	-0.2382	-2.1393	1.4584	H	-0.2882	2.0231	-1.0459	$\Delta E = -1.610$ kcal/mol			
H	1.2575	-1.3009	0.9609	N	1.5327	-0.0018	1.8898	C	-0.3543	-0.0013	-2.7689
H	-0.2369	2.1440	1.4751	O	-0.3881	-0.0025	-1.0182	C	-0.0863	-1.1785	0.5812
H	1.2536	1.3083	0.9576	[LPd-C(O)...O(CH ₃) ₂] ²⁺				C	-0.0861	1.1774	0.5790
H	0.8084	1.3183	2.6616	$\Delta E = -17.69$ kcal/mol				H	0.1257	-1.2311	1.6565
O	-1.5348	0.0038	1.1128	C	1.7217	-1.0592	2.8471	H	0.8644	-1.2252	0.0355
O	0.4625	-0.0011	-1.4088	C	1.3213	1.2223	3.3824	H	-0.7043	-2.0290	0.2954
				C	-1.5191	-0.1063	2.3447	H	0.1268	1.2314	1.6540
				C	-0.5269	1.1594	-2.1158	H	-0.7043	2.0275	0.2924
				C	-0.7390	2.2727	-1.1771	H	0.8642	1.2232	0.0324
				C	-0.5187	-1.2010	-2.1537	O	0.7606	0.0063	-2.6151
				C	-0.7242	-2.3451	-1.2531	O	-0.8066	-0.0008	0.2577
				C	-0.2395	1.2123	-3.4764				
				C	-0.2315	-1.2124	-3.5148				
				C	-0.0936	0.0110	-4.1718				
				H	1.4188	-1.4030	3.8408				
				H	2.8034	-0.9028	2.8368				
				H	1.4667	-1.8156	2.1052				
				H	1.0127	0.9786	4.4032				
				H	0.7664	2.0933	3.0353				
				H	2.3894	1.4535	3.3751				
				H	-1.1642	2.7414	0.6815				
				H	-1.1463	-2.8789	0.5893				
				H	-0.6661	3.3055	-1.5091				
				H	-0.6515	-3.3661	-1.6203				
				H	-0.1344	2.1632	-3.9820				
				H	-0.1213	-2.1476	-4.0485				
				H	0.1265	0.0279	-5.2316				
				N	-1.0160	1.9673	0.0381				
				N	-0.9973	-2.0826	-0.0265				
				N	-0.6543	-0.0311	-1.5138				
				O	-1.8470	-0.1333	3.4148				
				O	1.0354	0.1429	2.4856				
				Pd	-1.0714	-0.0662	0.4144				

Table S2. Numerical breakdown of a topological analysis of the metal bound carbon monoxide ligands present in the CSD. As is evident from entries 1-5, virtually all carbon monoxide ligands in the CSD are η^1 -coordinated. Moreover, the majority of data involved metals with multiple CO ligands (entries 6-11). In about 60 % of all CIFs, three or more CO ligands are present (i.e. 28,597, see entry 7). Relatively few structures contain CO as the sole ligand, as is indicated in entries 12-16. As is detailed in entries 17-31, there is a large variety in the amount of atoms that are bound to metal in M-CO structures with $t=2$ up to $t=14$. These large t -values are a result of ligands that bind in a polytopic fashion such as η^2 -acetylene (Ac), η^2 -ethylene (Et), η^5 -cyclopentadienyl (Cp) and η^6 -benzene (Bn). A specification of structures and geometries that contain only monotopic (η^1) ligands is listed in entries 32-39. Octahedral structures are by far the most abundant (15,312 CIFs, entry 39) far the most abundant geometry, followed by trigonal bipyramidal (1,822 CIFs, entry 38) and square planar complexes (1,689 CIFs, entry 35). The geometries with the multitopic ligands Ac, Et, Cp, and Bn were analyzed separately, considering structures of the type ML_4 (entries 40-43), ML_5 (entries 44-47) and ML_6 (entries 48-51). Finally, the geometries of $L_nM\cdots(C\equiv O)_3$ complexes was analyzed (entries 52-62), revealing that octahedral (11,264 CIFs, entry 58) and pianostool-like complexes (2,913 CIFs, entries 61 and 62) constitute most of the data.

Entry	Query ^a	CIFs	Entry	Query ^a	CIFs
Hapticity of CO ligands:			Geometry of $L_nM\cdots C\equiv O$ complexes		
1	$M\cdots C\equiv O$ (η^1)	48,019	32	$n = 2^c$	8
2	$M_2\cdots C\equiv O$ (η^2)	9	33	$n = 3^c$	36
3	$M_3\cdots C\equiv O$ (η^3)	3	34	$n = 4^{\text{tetrahedral, d}}$	344
4	$M_4\cdots C\equiv O$ (η^4)	0	35	$n = 4^{\text{square planar, e}}$	1,689
5	$M_5\cdots C\equiv O$ (η^5)	0	36	$n = 5^{\text{planar pentagonal, f}}$	175
Number of CO ligands bound to the same metal:			37	$n = 5^{\text{square pyramidal, g}}$	541
6	$L_nM\cdots(C\equiv O)_2$	39,389 (10,792) ^b	38	$n = 5^{\text{trigonal bipyramidal, h}}$	1,822
7	$L_nM\cdots(C\equiv O)_3$	28,597 (18,979) ^b	39	$n = 6^{\text{octahedral, i}}$	15,312
8	$L_nM\cdots(C\equiv O)_4$	9,618 (5,709) ^b	Geometry of $PL_nM\cdots C\equiv O$ complexes (P = π-donor ligand)^l		
9	$L_nM\cdots(C\equiv O)_5$	3,909 (3,861) ^b	40	$n = 2, P = \text{Ac}$ (ML_4)	24
10	$L_nM\cdots(C\equiv O)_6$	48 (48) ^b	41	$n = 2, P = \text{Et}$ "	24
11	$L_nM\cdots(C\equiv O)_7$	0	42	$n = 2, P = \text{Cp}^k$ "	4,351
Structures where CO is the only ligand			43	$n = 2, P = \text{Bn}^k$ "	1,532
12	$M\cdots(C\equiv O)_2$	2	44	$n = 3, P = \text{Ac}^l$ (ML_5)	764
13	$M\cdots(C\equiv O)_3$	0	45	$n = 3, P = \text{Et}^l$ "	280
14	$M\cdots(C\equiv O)_4$	100	46	$n = 3, P = \text{Cp}^k$ "	3,193
15	$M\cdots(C\equiv O)_5$	37	47	$n = 3, P = \text{Bn}^k$ "	68
16	$M\cdots(C\equiv O)_6$	42	48	$n = 4, P = \text{Ac}^m$ (ML_6)	473
Number of atoms bonded to M in $M\cdots C\equiv O$ (t)			49	$n = 4, P = \text{Et}^m$ "	1,682
17	$t = 1$	0	50	$n = 4, P = \text{Cp}^{k,n}$ "	1,513
18	$t = 2$	8	51	$n = 4, P = \text{Bn}^{k,n}$ "	11
19	$t = 3$	36	Geometry of $L_nM\cdots(C\equiv O)_3$ complexes^o		
20	$t = 4$	2,355	52	$L_nM\cdots(C\equiv O)_3$ (= entry 7)	28,597
21	$t = 5$	2,570	53	$LM\cdots(C\equiv O)_3^{\text{tetrahedral, d}}$	183
22	$t = 6$	25,145	54	$LM\cdots(C\equiv O)_3^{\text{square planar, e}}$	4
23	$t = 7$	10,296	55	$L_2M\cdots(C\equiv O)_3^{\text{planar pentagonal, f}}$	0
24	$t = 8$	10,014	56	$L_2M\cdots(C\equiv O)_3^{\text{square pyramidal, g}}$	21
25	$t = 9$	6,426	57	$L_2M\cdots(C\equiv O)_3^{\text{trigonal bipyramidal, h}}$	938
26	$t = 10$	2,023	58	$L_3M\cdots(C\equiv O)_3^{\text{octahedral}}$	11,264
27	$t = 11$	440	59	$\text{Ac}M\cdots(C\equiv O)_3$	949
28	$t = 12$	141	60	$\text{Et}M\cdots(C\equiv O)_3$	1,735
29	$t = 13$	22	61	$\text{Cp}M\cdots(C\equiv O)_3$	1,549
30	$t = 14$	3	62	$\text{Bn}M\cdots(C\equiv O)_3$	1,364
31	$t = 15$	0			

^a O is always bound to only one atom, the CO ligand is η^1 coordinated unless otherwise specified and L stands for any other monoatomic ligand; ^b Amount of CIFs found with the structure indicated in the entry, minus the amount of CIFs of structure with one additional CO ligand (two rows down); ^c exact geometry not specified; ^d all L-M-L angles were constrained to $109.5 \pm 9^\circ$; ^e two trans L-M-L angles were constrained to $160-180^\circ$; ^f All L-[ML_3]^{plane} distances were confined to $0 \pm 1 \text{ \AA}$; ^g the trans L-M-L angles of equatorial ligands were constrained to $160-180^\circ$ and one L-M-L angle with the axial ligand was confined to $20 - 160^\circ$. A CO ligand is axial in 71 CIFs and equatorial in 470 CIFs; ^h the trans L-M-L angle of axial ligands was constrained to $160-180^\circ$ and the three L-M-L angles with the equatorial ligands was confined to $120 \pm 10^\circ$. A CO ligand is axial in 771 CIFs and equatorial in 1051 CIFs; ⁱ the three trans L-M-L angles were constrained to $160-180^\circ$; ^j the number of atoms bonded to M was set under the assumption that all atoms of π -ligand were bound. The π -ligand considered where (substituted) acetylene (Ac, 1,697 CIFs), ethylene (Et, 3,394 CIFs), cyclopentadienyl (Cp, 9,507 CIFs) and benzene (Bn, 1,639 CIFs) (allyl = 1522 cifs). There were 159 CIFs where $n = 0$ or 1 ; ^k piano-stool complexes; ^l tetrahedral and square planar complexes (nearly all cis); ^m octahedral complexes, polynuclear clusters and complexes with an allyl ligand; ⁿ mostly polynuclear clusters and complexes with an allyl ligand; ^o There are also 415 CIFs with an allyl ligand, making a total of 18,422 CIFs found with the indicated geometry. The remaining 10,175 CIFs likely involve clusters;

Table S3. Numerical overview of the nature of the possibly interacting electron rich atom (EIR) found in the database for the analysis with M-CO and M(CO)₃ structures (see also Figure 3).

EIR	M-C(O)···EIR		M-(CO) ₃ ···EIR	
	<i>N</i>	%	<i>N</i>	%
N	35,737	4.9	7,962	2.8
O	599,381	83	252,753	88
F	37,752	5.2	12,574	4.4
P	5,217	0.7	903	0.3
S	14,697	2.0	3,770	1.3
Cl	24,713	3.4	6,874	2.4
As	480	0.1	131	0.1
Se	1,670	0.2	309	0.1
Br	3,250	0.5	968	0.3
Te	916	0.1	154	0.1
I	1,974	0.3	423	0.2
At	0	0	0	0.0
Total	725,787	100	286,821	100

Table S4. Energies in kcal/mol of the complexes highlighted in Figure 4 and Figure S5 computed with DFT at the B3LYP-D3/def2-TZVP level of theory (ΔE^1). At this level of theory the methane and water dimers have an energy of respectively – 0.57 and –6.32 kcal/mol (coordinates not given). For the structures highlighted in Figure 4 an additional fragment analysis was conducted with ADF giving ΔE^2 .

CSD entry	With	ΔE^1 , ^a	ΔE^2 , ^b	PR ^c	EA ^c	OI ^c	DS ^c
HAVKAQ	sp O-atom	-20.76 ^d	-38.96 ^e	10.23	-20.6	-8.92	-19.67
ACUZII	sp ² O-atom	-8.80					
ACUZII01	sp ² O-atom	-8.49	-8.39	7.47	-7.45	-2.56	-5.85
HIDSIW	sp ² O-atom	-8.23					
PYRMNC	sp ² O-atom	-7.92					
QENCOC	sp ² O-atom	-7.41					
MOPZUO	sp ³ O-atom	-11.17 ^d					
NOFRUW	sp ³ O-atom	-10.42 ^d					
VUWKED	sp ³ O-atom	-9.05	-8.18	10.84	-8.12	-2.63	-8.27
PUNCOS	Cl ⁻	-88.20	-84.35	21.42	-81.55	-20.24	-3.98
CEHHIH	BF ₄ ⁻	-154.98					
CEHHON	BF ₄ ⁻	-155.67					
CUWYOI01	BF ₄ ⁻	-55.91 ^f					
CUWYOI01	BF ₄ ⁻	-56.10 ^g					
DUSYIZ	BF ₄ ⁻	-63.39					
GOZYOJ	BF ₄ ⁻	-139.70	-138.54	6.02	-131.4	-10.08	-3.08
VOTJAP	BF ₄ ⁻	-64.10					
HOLMOK	SbF ₆ ⁻	-135.07					
LARPIE	SbF ₆ ⁻	-134.71	-133.16	9.63	-121.74	-13.99	-7.06
LARPOK	SbF ₆ ⁻	-134.48					

^a ΔE^1 was computed by single point energy computation of the geometries lifted from the CSD of the complex minus those of the complex without anion and the anion. ^b ΔE^2 was obtained by a similar single point calculation with ADF at the B3LYP-D3/TZ2P level of theory (no frozen cores and scalar relativity); ^c Results of an ADF fragment analysis with the total bonding energy (ΔE^2) split up into the Pauli repulsion (PR), electrostatic attraction (EA), orbital interactions (OI) and dispersion (DS). ^d Energy computed at B3LYP-D3/6-31G* level of theory due to the large cluster involved. ^e Energies computed at GGA:BP-D3(BK)/DZ level of theory due to the large cluster involved. ^f In the complex concerned the three CO ligands are staggered with respect to the CP*'s methyl groups. ^g In the complex concerned the three CO ligands are eclipsed with respect to the CP*'s methyl groups.